Morbidity and Mortality of Mechanical Thrombectomy in relation to age

Thesis

Submitted for Partial fulfillment of MD Degree in Radiology

By

Mohamed Elsayed Salem Sowelm
M.B.B.Ch, Ain shams University

Under supervision of

Prof. Dr. Mostafa Mahmoud Gamal Eldin
Professor of Diagnostic & interventional Radiology
Faculty of Medicine Ain Shams University

Prof. Dr. Amr Mahmoud Ahmed
Professor of Diagnostic & interventional Radiology
Faculty of Medicine Ain Shams University

Dr. Mostafa Mohamed Farid
Lecturer of Diagnostic & interventional Radiology
Ain Shams University

Faculty of Medicine
Ain -shams University
2022

بسم الله الرحمن الرحيم

قالوا

سبحانك لا علم لنا
إلا ما علمتنا إنك أنت
العليم الحكيم

صدق الله العظيم

سورة البقرة الآية: ٣٢

Acknowledgement

First of all, thanks to **Allah** whose magnificent help was the mainfactor in completing this work.

I would like to express my deepest gratitude and thanks to **Prof. Dr. Mostafa Mahmoud Gamal Eldin**, Professor of Diagnostic & interventional Radiology, Faculty of Medicine, Ain Shams University, For giving me the honor of being her candidate, working under her supervision, guided by her experience and precious advices and true concern, I could not ask for a better mentor and role model.

Words could not express my appreciation, thanks and respect to**Prof. Dr. Amr Mahmoud Ahmed**, Professor of Diagnostic & interventional Radiology, Faculty of Medicine, Ain Shams University, for his kindness, patience, consideration, precious assistance throughout this work.

I would like to express my deepest gratitude and thanks to **Dr. Mostafa Mohamed Farid**, Lecturer of Diagnostic & interventional Radiology, Faculty of Medicine, Ain Shams University, To be given the honor of working under his guidance, guided by his experience, precious advice and genuine interest, I could not have asked for a better teacher and role model.

Mohamed Elsayed Salem Sowelm

List of Contents

Title	Page No.
List of Contents	I
List of Abbreviations	II
List of Tables	III
List of Figures	IV
Introduction	1
Aim of the Work	2
Review of Literature	3
Anatomy of the cerebral circulation	3
Stroke	59
METHODOLOGY	100
RESULTS	107
Case Presentation	117
Discussion	131
LIMITATIONS	137
Conclusion& Recommendations	138
Summary	139
References	141

List of Abbreviations

Abb.		Full Term
± SD		Standard deviation
AASLD	**:**	American Association for the Study of Liver Diseases
ADC	**:**	Apparent diffusion coefficient
AUC		Area under curve
BB-EPI	**:**	Black-blood echo planar
BCLC	**:**	Barcelona Clinic Liver Cancer
CA	**:**	contrast agents

List of Tables

Table No.	Title	Page

Table (1): Sources of asymmetry in the circle of Willis (Harrigan and Deveikis, 2013). 27

Table (2): distribution of MRS scores in both age groups........................113

Table (3): distribution of TICI scores in both age groups........................114

List of Figures

Fig No.	Title	Page
Fig (1):	Common aortic arch configurations.	4
Fig (2):	Selected aortic arch anomalies.	5
Fig (3):	Selected segmental classification schemes of the internal carotid artery	6
Fig (4):	Carotid–vertebrobasilar anastomoses.	9
Fig (5):	Cavernous internal carotid artery.	12
Fig (6):	Inferolateral trunk.	15
Fig (7):	Clinoidal segment.	16
Fig (8):	Ophthalmic artery.	21
Fig (9):	Persistent fetal configuration of the posterior communicating artery.	23
Fig (10):	Posterior communicating artery infundibulum	24
Fig (11):	Circle of Willis	27
Fig (12):	Anterior cerebral artery. Left lateral oblique view of the left ACA	28
Fig (13):	Artist's impression of the anterior circle of Willis showing lenticulostriate arteries arising from the anterior cerebral arteries (*M* medial group) and middle cerebral artery (*L* lateral group).	30
Fig (14):	Anterior communicating artery complex. In most cases, ACom complex assumes one of the four configurations.	32
Fig (15):	Distal branches of the anterior cerebral artery	35
Fig (16):	MCA segments	37
Fig (17):	MCA cortical branches.	40
Fig (18):	The vertebral artery	42
Fig (19):	Posterior inferior cerebellar artery. Lateral view of the brainstem and cerebellum.	46
Fig (20):	Posterior cerebral artery.	48
Fig (21):	Major branches of the posterior cerebral artery.	51
Fig (22):	The PCA pitchfork.	56
Fig (23):	Penumbra. At baseline a small infarct core is already manifest, and a larger surrounding area is at risk (penumbra)	60
Fig (24):	Circle of Willis (Bottom view of brain).	62
Fig (25):	Pial collaterals. Carotid artery angiogram in frontal projection.	62
Fig (26):	Axial CT images of the brain. Note dense vessel sign of the left middle cerebral artery (left image) and the loss of grey-white matter differentiation around the left putamen (middle image). No signs of infarction in the right image.	64
Fig (27):	CT angiography. Occlusion of the left middle cerebral artery (right side in each image). The arteries in the left hemisphere, seen beyond the occlusion, are supplied in retrograde direction via the anterior and posterior cerebral arteries (collateral flow).	66
Fig (28):	CT perfusion, attenuation of contrast medium measured in Hounsfield Units (HU) plotted against time, describing the different parameters used.	68
Fig (29):	CT perfusion images.	68
Fig (30):	MRI at the level of pons and cerebellum.	70

Fig (31): The National Institutes of Health Stroke Scale, NIHSS. 72
Fig (32): Glasgow Coma Scale, GCS. 73
Fig (33): The ten included areas of ASPECTS. C – Caudate nucleus, L - Lentiform nucleus, IC - Internal Capsule, I – Insular cortex, M1, M2, M3 - middle cerebral artery territory at the level of the basal ganglia, M4, M5, and M6 - middle cerebral artery territory at the level of cella media and above. 73
Fig (34): Modified Treatment in Cerebral Ischemia Scale, mTICI. 76
Fig (35): The modified Rankin Scale, mRS.. 76
Fig (36): The Amplatz GooseNeck Snare.. 88
Fig (37): The Merci Retriever.*.. 88
Fig (38): The Penumbra separators and aspiration pump. 90
Fig (39): The Solitaire device (above) and the Trevo device (below). 91
Fig (40): Box-and-whisker plot of the patients' ages in the study. Whiskers represent range, bars represent the 25th and 75th percentiles and lines represent median values. 107
Fig (41): Clustered column chart showing the distribution of males and females in both age groups 108
Fig (42): Clustered column chart showing the site of the occluded artery in both age groups 108
Fig (43): Clustered column chart showing the number of smokers and non-smokers in both age groups 109
Fig (44): Clustered column chart showing the number of hypertensive and normotensive patients in both age groups 109
Fig (45): Clustered column chart showing the number of diabetic and non-diabetic patients in both age groups 110
Fig (46): Clustered column chart showing the number of patients with and without coronary heart disease in both age groups 110
Fig (47): Clustered column chart showing the number of patients with and without dyslipidemia in both age groups.. 111
Fig (48): Clustered column chart showing the number of patients with and without TIAs in both age groups 111
Fig (49): Clustered column chart showing the distribution of a favorable outcome as designated by a MRS score of ≤ 2 in both age groups 112
Fig (50): Clustered column chart showing the distribution of the MRS scores in both age groups 113
Fig (51): Clustered column chart showing the distribution of successful recanalization as designated by a TICI scale score of ≥ 2b in both age groups 114
Fig (52): Clustered column chart showing the distribution of the TICI scale scores in both age groups 115
Fig (53): Clustered column chart showing the incidence of futile recanalization in both age groups 115
Fig (54): Clustered column chart showing the incidence of post-procedural hemorrhage in both age groups 116

Introduction

Intracranial mechanical thrombectomy is a promising ischemic stroke treatment. There is ongoing interest in the selection of appropriate candidates because it remains unclear which patients benefit the most. The elderly population is predicted to double in a half century, and it is well established that older persons have a higher risk of stroke. **(Brown RD et al., 2005).**

Advanced age also carries with it the burden of decreased neuronal plasticity and an ever-decreasing pool of healthy neurons. A large intracranial vessel occlusion may irreversibly injure a higher proportion of neurons in an elderly patient than it would in a younger patient under similar circumstances, substantially impeding recovery of neurologic function. Thus, elderly patients may incur more disability regardless of treatment technique. **(Arnold M et al., 2008).**

It is critical to investigate the benefit of newer treatments and to understand potential characteristics within this population, which may influence clinical outcome following endovascular therapy (ET). The aim of this substudy was to examine the influence of age on clinical and revascularization outcomes. **(Zaidat oo et al., 2014).**

In this study we assessed the cost and benefit balance of mechanical thrombectomy for acute ischemic stroke in patients with large cerebral artery occlusion with the first six hours of symptoms onset in relation to the age.

Aim of the Work

The study aim to explore the efficacy of mechanical thrombectomy ,with respect to increasing patient age.

In this way we hoped to be able to assess the value of the technique in this age group to get the maximum benefit from it.

Review of Literature

Chapter 1

Anatomy of the cerebral circulation

The blood supply to the brain is provided by two arterial axes on each side of the neck, i.e. the internal carotid and vertebral arteries **(Osborn, 1999)**.

Aortic Arch and Great Vessels:

Aortic arch anatomy is pertinent to neuroangiography because variations of arch anatomy can affect access to the cervicocranial circulation:

1) ***Branches* (Figure 1a):**

   a) Innominate (aka brachiocephalic) artery.

   b) Left common carotid artery.

   c) Left subclavian artery **(Osborn, 1999)**.

2) ***Variants* (Figure 1):**

a) Bovine arch **(Figure 1b)**. The innominate artery and left common carotid artery (CCA) share a common origin (up to 27% of cases), or the left CCA arises from the innominate artery (7% of cases). The bovine variant is more common in blacks (10–25%) than whites (5–8%) **(Osborn, 1999)**.

b) Aberrant right subclavian artery **(Figure 1d)**. The right subclavian artery arises from the left aortic arch, distal to the origin of the left subclavian artery. It usually passes posterior to the esophagus on its way to the right upper extremity. This is the most common congenital arch anomaly; incidence: 0.4 – 2.0%, 0.3% It is associated with Down syndrome **(Harrigan and Deveikis, 2013)**.

c) Origin of the left vertebral artery from the arch is seen in 0.5% of cases **(Figure 1c) (Harrigan and Deveikis, 2013)**.

d) Less common variants **(Figure 2)**. Some of these rare anomalies can lead to formation of a vascular ring in which the trachea and esophagus are encircled by connecting segments of the aortic arch and its branches **(Harrigan and Deveikis, 2013)**.

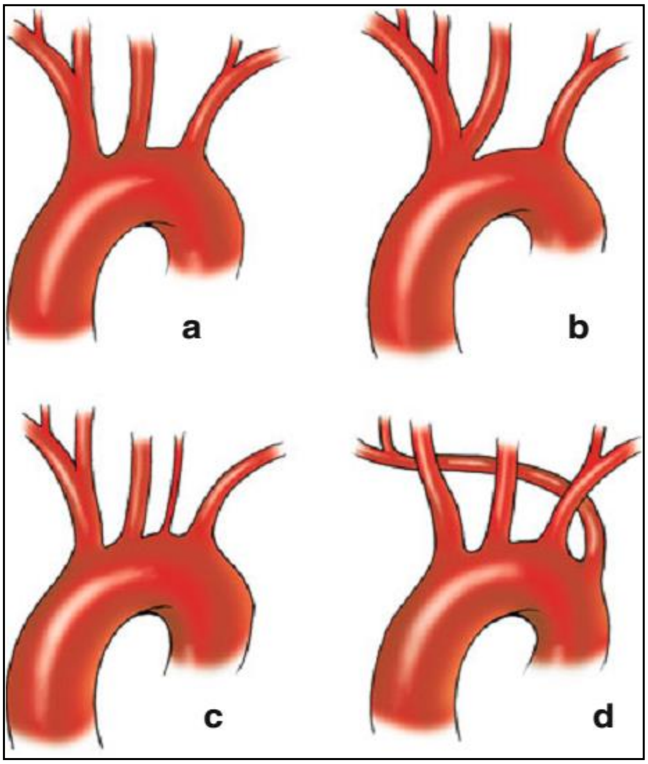

Fig (1): Common aortic arch configurations. Clockwise from upper left: (a) Normal arch; (b) bovine arch; (c) origin of the left vertebral artery from the arch, and (d) aberrant right subclavian artery ***(Harrigan and Deveikis, 2013).***

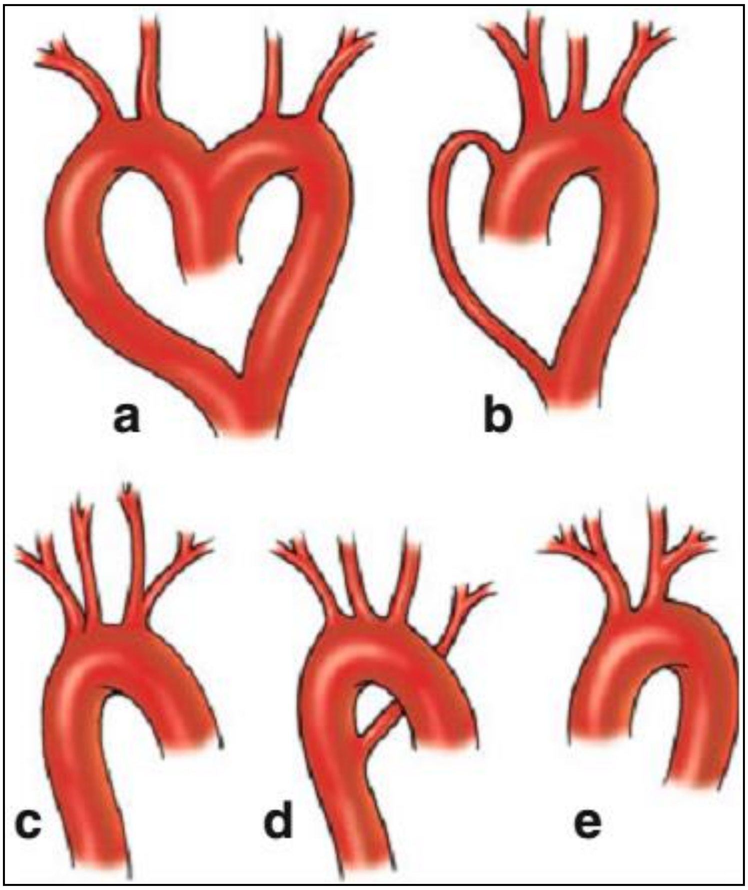

Fig (2): Selected aortic arch anomalies. (a) Double aortic arch. The arches encircle the trachea and esophagus to form the descending aorta, which is usually on the left. The right arch is larger than the left in up to 75% of cases. (b) Double aortic arch with left arch atresia. (c) Right aortic arch with a mirror configuration. The descending aorta is on the right side of the heart. This anomaly does not form a vascular ring, but is associated with other anomalies such as tetralogy of Fallot1. (d) Right aortic arch with a non-mirror configuration and an aberrant left subclavian artery. The descending aorta is on the right side of the heart, and the left subclavian artery arises from the proximal aorta. A common cause of a symptomatic vascular ring. (e) Bi innominate artery ***(Harrigan and Deveikis, 2013).***

Common Carotid Artery:

The CCAs travel within the carotid sheath, which also contains the internal jugular vein and the vagus nerve. The right CCA is usually shorter than the left. The CCAs typically bifurcate at the C3 or C4 level (upper border of the thyroid cartilage), although the bifurcation may be located anywhere between T2 and C2. The CCAs do not usually have